Multimetallocenes. A Theoretical Study

Alejandro Velazquez,[†] Israel Fernández,[‡] Gernot Frenking,*[,‡] and Gabriel Merino*[,†]

Facultad de Química, Universidad de Guanajuato, Noria Alta s/n, CP 36050, Guanajuato, Gto, México, and Department of Chemistry, Philipps-University Marburg, Hans-Meerwein-Strasse, D-35042 Marburg, Germany

Received May 14, 2007

Quantum chemical calculations using gradient-corrected density functional theory at the BP86 level in conjunction with TZ2P basis sets have been carried out for the multimetallocenes CpM_nCp, where M = Be, Mg, Ca, and Zn with $n = 2-5$. The equilibrium geometries and energetics with respect to loss of one metal atom are theoretically predicted. The nature of the metal−ligand interactions between the M_n^{2+} and $(Cp^-)_2$ moieties was investigated with energy decomposition analysis (EDA). The calculations predict that the CpM_nCp species with $n > 2$ are thermodynamically unstable with respect to loss of one metal atom except for the beryllium compounds. The beryllocenes exhibit unusual stabilities in the gas phase for the whole series $CpBe_nCp$ up to $n = 5$. The calculations suggest that the energy for loss of one metal atom from $CpBe_2Cp$ is significantly higher than from $CpZn_2Cp$. The energy for the metal extrusion reaction of $CpBe_3Cp$ is much less endothermic than for $CpBe_2Cp$ but it is still more endothermic than the reaction of $CpZn_2Cp$. The thermodynamic stability of the higher members $CpBe_4Cp$ and $CpBe_5Cp$ toward loss of one metal atom is only slightly less than for $CpBe_3Cp$, while the other multimetallocenes, CpM_3Cp, CpM_4Cp, and CpM_5Cp (M = Mg, Ca, Zn), possess little extra stabilization with respect to the dimetallocenes. The calculated reaction energies which include the heats of sublimation of the metals indicate that $CpBe_2Cp$ might become isolated in the condensed phase, while the prospect for $CpCa_2Cp$ and $CpMg_2Cp$ and for the higher members CpM_3Cp, CpM_4Cp, and CpM_5Cp is less likely. The analysis of the metal−ligand bonding in CpM_nCp using the EDA method suggests that the interactions between M_n^{2+} and $(Cp^-)_2$ have a larger electrostatic than covalent character. The beryllocenes are more covalently bonded than the other multimetallocenes. The orbital interactions in the lower members of CpM_nCp come mainly from π orbitals, but the σ contribution continuously increases when n becomes larger and eventually may become stronger than the π contributions, which become weaker in the higher members of the series.

Introduction

The synthesis of the first stable molecular compound containing a Zn−Zn bond unsupported by bridging ligands (decamethyldizincocene) was reported by Carmona and co-workers in 2004.[1] The crystal structure of decamethyldizincocene reveals a pair of zinc atoms which are sandwiched between two permethylcyclopentadienyl rings (Cp*) in such a way that the Zn−Zn bond is collinear with the C_5 axes of the organic rings. The discovery of the dizincocene, the first dimetallocene, has triggered the interest of several experimental and theoretical groups in finding analogous compounds $Cp^*_2M_2$, where M is any metal other than zinc.[2−21] Until today the search for stable species with the formula $Cp^*_2M_2$ has not been successful except for M = Zn. However, there is a related question regarding the change of element M which has not been addressed so far: How many atoms M_n can be sandwiched by two Cp* rings, yielding a stable multimetallocene, $Cp^*_2M_n$? Is it possible that multimetallocene compounds may become synthesized? To give an answer to this question, we carried out quantum chemical calculations on a series of multimetallocenes with the formula

* To whom correspondence should be addressed. E-mail: gmerino@quijote.ugto.mx (G.M.); frenking@chemie.uni-marburg.de (G.F.).
† Universidad de Guanajuato.
‡ Philipps-University Marburg.

(1) Resa, I.; Carmona, E.; Gutiérrez-Puebla, E.; Monge, A. *Science* **2004**, *305*, 1136.
(2) Kan, Y. H. *J. Mol. Struct.: THEOCHEM* **2007**, *805*, 127.
(3) Álvarez, E.; Grirrane, A.; Resa, I.; del Río, D.; Rodríguez, A.; Carmona, E. *Angew. Chem., Int. Ed.* **2007**, *46*, 1296.
(4) Grirrane, A.; Resa, I.; Rodríguez, A.; Carmona, E.; Álvarez, E.; Gutíerrez-Puebla, E.; Monge, A.; Galindo, A.; del Río, D.; Andersen, R. A. *J. Am. Chem. Soc.* **2007**, *129*, 693.
(5) Zhu, Z. L.; Fischer, R. C.; Fettinger, J. C.; Rivard, E.; Brynda, M.; Power, P. P. *J. Am. Chem. Soc.* **2006**, *128*, 15068.
(6) Li, Q. S.; Xu, Y. *J. Phys. Chem. A* **2006**, *110*, 11898.
(7) Wang, H. M.; Yang, C. L.; Wan, B. S.; Han, K. L. *J. Theor. Comput. Chem.* **2006**, *5*, 461.
(8) Xiu, H. Z.; Se, L.; Qian, S. L. *J. Theor. Comput. Chem.* **2006**, *5*, 475.
(9) Zhu, Z. L.; Wright, R. J.; Olmstead, M. M.; Rivard, E.; Brynda, M.; Power, P. P. *Angew. Chem., Int. Ed.* **2006**, *45*, 5807.
(10) Liu, Z. Z.; Tian, W. Q.; Feng, J. K.; Zhang, G.; Li, W. Q.; Cui, Y. H.; Sun, C. C. *Eur. J. Inorg. Chem.* **2006**, 2808.
(11) Zhou, J.; Wang, W. N.; Fan, K. N. *Chem. Phys. Lett.* **2006**, *424*, 247.
(12) Merino, G.; Beltran, H. I.; Vela, A. *Inorg. Chem.* **2006**, *45*, 1091.
(13) Richardson, S. L.; Baruah, T.; Pederson, M. R. *Chem. Phys. Lett.* **2005**, *415*, 141.
(14) Wang, Y. Z.; Quillian, B.; Wei, P. R.; Wang, H. Y.; Yang, X. J.; Xie, Y. M.; King, R. B.; Schleyer, P. V.; Schaefer, H. F.; Robinson, G. H. *J. Am. Chem. Soc.* **2005**, *127*, 11944.
(15) Kress, J. W. *J. Phys. Chem. A* **2005**, *109*, 7757.
(16) Timoshkin, A. Y.; Schaefer, H. F. *Organometallics* **2005**, *24*, 3343.
(17) Kang, H. S. *J. Phys. Chem. A* **2005**, *109*, 4342.
(18) Xie, Y. M.; Schaefer, H. F.; King, R. B. *J. Am. Chem. Soc.* **2005**, *127*, 2818.
(19) Xie, Z. Z.; Fang, W. H. *Chem. Phys. Lett.* **2005**, *404*, 212.
(20) del Río, D.; Galindo, A.; Resa, I.; Carmona, E. *Angew. Chem., Int. Ed.* **2005**, *44*, 1244.
(21) Xie, Y. M.; Schaefer, H. F.; Jemmis, E. D. *Chem. Phys. Lett.* **2005**, *402*, 414.

10.1021/om700477b CCC: $37.00
Publication on Web 08/11/2007

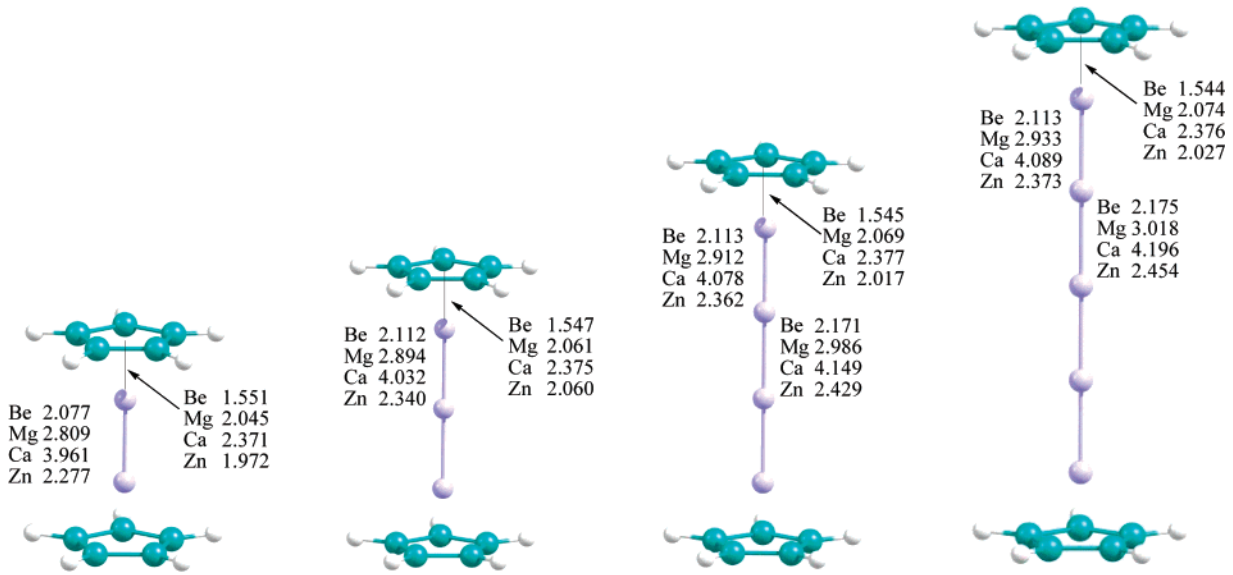

Figure 1. Optimized equilibrium geometries of multimetallocenes at the BP86/TZ2P level. The selected bond lengths are in angstroms.

CpM_nCp (M = Be, Mg, Ca, Zn; $n = 2-5$). We think that the substitution of Cp* by Cp does not affect the validity of our results with respect to the stability of the multimetallocenes.

We present theoretically predicted geometries and the stabilities of the CpM_nCp compounds for different n values. We also investigate the metal−Cp interactions using energy decomposition analysis (EDA). Our results may serve as a guideline for future experiments. To the best of our knowledge, this is the first theoretical study of compounds CpM_nCp where $n > 2$.

Methods

The geometries of the molecules were optimized at the gradient-corrected DFT level using Becke's exchange functional[22] in conjunction with Perdew's correlation functional[23] (BP86). Uncontracted Slater-type orbitals (STOs) were employed as basis functions in SCF calculations.[24] Triple-ζ-quality basis sets were used, which were augmented by two sets of polarization functions, that is, p and d functions for the hydrogen atom and d and f functions for the other atoms. This level is denoted as BP86/TZ2P. An auxiliary set of s, p, d, f, and g STOs was used to fit the molecular densities and to represent the Coulomb and exchange potentials accurately in each SCF cycle.[25] Scalar relativistic effects were considered using the zeroth-order regular approximation (ZORA).[26] Calculation of the vibrational frequencies at the optimized geometries showed that the compounds are minima on the potential energy surface. The calculations were carried out using the ADF(2006.1) program package.[27]

In EDA, bond formation between the interacting fragments is divided into three steps, which can be interpreted in a plausible way. In the first step the fragments, which are calculated with the frozen geometry of the entire molecule, are superimposed without electronic relaxation, yielding the quasiclassical electrostatic attraction ΔE_{elstat}. In the second step the product wave function becomes antisymmetrized and renormalized, which gives the repulsive term ΔE_{Pauli}, termed Pauli repulsion. In the third step the molecular orbitals relax to their final form to yield the stabilizing orbital interaction ΔE_{orb}. The latter term can be divided into contributions of orbitals having different symmetries. The sum of the three terms $\Delta E_{elstat} + \Delta E_{Pauli} + \Delta E_{orb}$ gives the total interaction energy ΔE_{int}:

$$\Delta E_{int} = \Delta E_{elstat} + \Delta E_{Pauli} + \Delta E_{orb}$$

Further details about EDA can be found in the literature.[27,28] Atomic partial charges were calculated using the NBO method using Gaussian 98.[29]

Results and Discussion

Figure 1 shows the optimized equilibrium structures of the multimetallocenes CpM_nCp and the most important M−M and M−X bond lengths, where X is the center of the Cp ring. The complete list of the geometrical data is given in the Supporting Information. In all cases, frequency calculations show that the eclipsed (D_{5h}) conformer is an energy minimum while the staggered (D_{5d}) conformer is a transition state. However, the energy differences between the D_{5h} and D_{5d} structures are

(22) Becke, A. D. *Phys. Rev. A* **1988**, *38*, 3098.
(23) Perdew, J. P. *Phys. Rev. B* **1986**, *33*, 8822.
(24) Snijders, J. G.; Baerends, E. J.; Vernooijs, P. *At. Nucl. Data Tables* **1982**, *26*, 483.
(25) Krijn, J.; Baerends, E. J. *Fit Functions in the HFSMethod*; Internal Report (in Dutch); Vrije Universiteit Amsterdam: Amsterdam, The Netherlands, 1984.
(26) (a) Chang, C.; Pelissier, M.; Durand, P. *Phys. Scr.* **1986**, *34*, 394. (b) Heully, J.-L.; Lindgren, I.; Lindroth, E.; Lundquist, S.; Martensson-Pendrill, A.-M. *J. Phys. Chem. B* **1986**, *19*, 2799. (c) van Lenthe, E.; Baerends, E. J.; Snijders, J. G. *J. Chem. Phys.* **1993**, *99*, 4597. (d) van Lenthe, E.; Baerends, E. J.; Snijders, J. G. *J. Chem. Phys.* **1996**, *105*, 6505. (e) van Lenthe, E.; van Leeuwen, R.; Baerends, E. J.; Snijders, J. G. *Int. J. Quantum Chem.* **1996**, *57*, 281.
(27) te Velde, G.; Bickelhaupt, F. M.; Baerends, E. J.; van Gisbergen, S. J. A.; Fonseca Guerra, C.; Snijders, J. G.; Ziegler, T. *J. Comput. Chem.* **2001**, *22*, 931.
(28) Recent reviews about the EDA method and its application have been published: (a) Bickelhaupt, F. M.; Baerends, E. J. *Rev. Comput. Chem.* **2000**, *15*, 1. (b) Lein, M.; Frenking, G. In *Theory and Applications of Computational Chemistry: The First 40 Years*; Dykstra, C. E., Frenking, G., Kim, K. S., Scuseria, G. E., Eds.; Elsevier: Amsterdam, 2005; p 291.
(29) (a) Reed, A. E.; Curtiss, L. A.; Weinhold, F. *Chem. Rev.* **1988**, *88*, 899. (b) Frisch, M. J.; Trucks, G. W.; Schlegel, H. B.; Scuseria, G. E.; Robb, M. A.; Cheeseman, J. R.; Zakrzewski, V. G.; Montgomery, J. A.; Stratmann, R. E.; Burant, J. C.; Dapprich, S.; Millan, J. M.; Daniels, A. D.; Kudin, K. N.; Strain, M. C.; Farkas, O.; Tomasi, J.; Barone, V.; Cossi, M.; Cammi, R.; Mennucci, B.; Pomelli, C.; Adamo, C.; Clifford, S.; Ochterski, J.; Petersson, G. A.; Ayala, P. Y.; Cui, Q.; Morokuma, K.; Malick, D. K.; Rabuck, A. D.; Raghavachari, K.; Foresman, J. B.; Cioslowski, J.; Ortiz, J. V.; Baboul, A. G.; Stefanov, B. B.; Liu, G.; Liashenko, A.; Piskorz, P.; Komaromi, I.; Gomperts, R.; Martin, R. L.; Fox, D. J.; Keith, T.; Al-Laham, M. A.; Peng, C. Y.; Nanayakkara, A.; Gonzales, C.; Challacombe, M.; Gill, P. M. W.; Johnson, B.; Chen, W.; Wong, M. W.; Andreas, J. L.; Head-Gordon, M.; Reploge, E. S.; Pople, J. A. *Gaussian 98*, revision A7; Gaussian Inc.: Pittsburg, PA, 1998.

Table 1. Calculated Data for HM_2H and CpM_2Cp (M = Be, Mg, Ca, Zn) Species at the BP86/TZ2P Level: Bond Lengths *r*(M−M) (Å), HOMO−LUMO Gap (eV), NBO Charges at the M_2 Fragment *q*(M_2)

compd	*r*(M−M)	HOMO−LUMO	*q*(M_2)[a]
HBe_2H	2.098	3.33	1.30
HMg_2H	2.884	2.72	1.40
HCa_2H	3.847	1.48	1.55
HZn_2H	2.404	3.68	1.20
$CpBe_2Cp$	2.077	4.33	1.70
$CpMg_2Cp$	2.809	3.87	1.80
$CpCa_2Cp$	3.961	1.76	1.75
$CpZn_2Cp$	2.277	4.49	1.85

[a] NBO analyses were done at the BP86/6-311G(d,p)//BP86/TZ2P level.

negligible (<0.1 kcal·mol^{-1}), which suggests that there is nearly free rotation of the organic ligands. The computed Zn−Zn distance is 2.277 Å, which is in good agreement with the experimental value of 2.305 Å for the Cp* homologue. The terminal M−M bonds in the tetra- and pentametallecenes are always slightly shorter than the central M−M bonds. Interestingly, the distance between the metal and the center of the Cp ring slightly increases from $n = 2$ to $n = 5$, except for the beryllium compounds.

Before presenting the results of the higher multimetallocenes, we want to shortly discuss the particular influence of the Cp ring on the compounds. To this end we compare the dimetallocenes CpM_2Cp with the dihydrides HM_2H. The zinc compound HZn_2H was previously studied with theoretical methods by Kaupp and von Schnering.[30] They predicted that HZn_2H should be an observable species in the gas phase, but experimental evidence is lacking so far. Table 1 gives the calculated M−M distances, the HOMO−LUMO gaps, and the atomic partial charges *q*(M). It becomes obvious that the CpM_2Cp species have shorter M−M distances than the HM_2H homologues with the notable exception of M = Ca. The metal atoms in CpM_2Cp carry a significantly higher positive charge than in HM_2H. The *q*(M) values indicate that it is reasonable to discuss the metal−Cp bonding in CpM_2Cp in terms of interactions between M_2^{2+} and $(Cp^-)_2$. Note that the HOMO−LUMO gap in the latter compounds is clearly larger than in the dihydrogen compounds.

The most important aspect of the multimetallocenes from an experimental point of view is the stability with respect to loss of metal atoms. To this end we calculated the energetics of the metal extrusion reaction 1. Reaction 1 is interesting since in

$$CpM_nCp \rightarrow CpM_{n-1}Cp + M \qquad (1)$$

several chemical processes described by Carmona and coworkers,[1] disproportionation of $Cp^*Zn_2Cp^*$ occurs, yielding a Zn(II)-containing species and elemental zinc. The fragmentation reaction 1 is an indirect way to estimate the stability of a multimetallocene. Figure 2 displays the trend of the calculated energies for reaction 1.[31−33] The results are striking. The removal of a metal from dimetallocene is an endothermic process particularly for diberyllocene (67.6, 14.2, 9.6, and 22.5 kcal·mol^{-1} for Be, Mg, Ca, and Zn, respectively), suggesting that the formation of dimetallocenes from monometallocenes is a favorable process. However, the scenario changes drastically when the number of metal atoms sandwiched by two Cp rings is higher than two. For the magnesium, calcium, and zinc complexes, the reaction energies for the disproportion reaction are close to zero, indicating that the formation of multimetallocenes CpM_nCp with $n > 2$ is not a favorable process. In contrast, the insertion reaction of an additional beryllium atom to the $CpBe_nCp$ complexes ($n = 2-4$) is exothermic by a rather constant value of 27 kcal·mol^{-1}. The results suggest that the formation of tri-, tetra-, and even pentaberyllocene from the precursor species is thermodynamically favored in the gas phase! This is a remarkable result. The very high reaction value for the formation of diberyllocene suggests that $Cp^*Be_2Cp^*$ might be even more stable than $Cp^*Zn_2Cp^*$. Furthermore, the beryllocenes $CpBe_nCp$ or $Cp^*Be_nCp^*$ are the only species of the metals which are investigated here for which compounds with $n > 2$ could become synthesized.

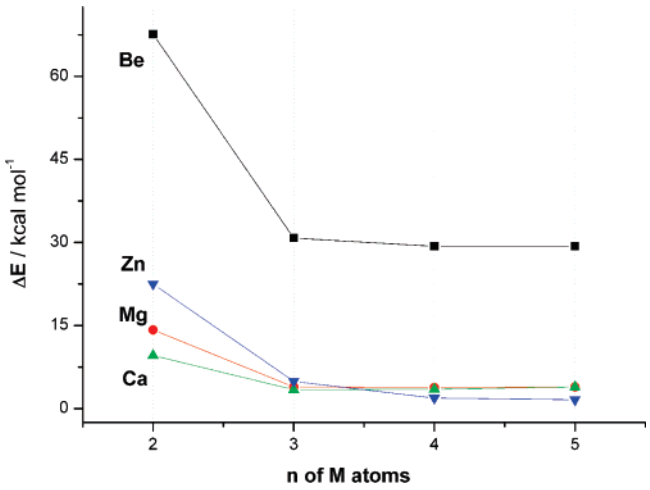

Figure 2. Energetics of the reaction $CpM_nCp \rightarrow CpM_{n-1}Cp + M$ at the BP86/TZ2P level (kcal·mol^{-1}).

Reaction 1 considers the formation of multimetallocenes in the gas phase. For the synthesis in the condensed phase it is necessary to consider reaction 2. The difference in the energetics

$$CpM_nCp(s) \rightleftarrows CpM_{n-1}Cp(s) + M(s) \qquad (2)$$

of reactions 1 and 2 is due to the sublimation enthalpies of all compounds. Since solid CpM_nCp and $CpM_{n-1}Cp$ have similar structures, one can assume similar intermolecular forces in the solid state. Thus, it is reasonable to expect that their sublimation enthalpies will be close to each other and their contribution in going from reaction 1 to 2 will be approximately the same. Therefore, the major contribution comes from the sublimation enthalpy of the metal M. Literature values of the sublimation enthalpies of Be, Mg, Ca, and Zn are 77.4, 35.2, 42.5, and 31.2 kcal·mol^{-1}, respectively.[34] Therefore, the enthalpies of reaction 2 for multimetallocenes will be more exothermic by approximately this amount compared to the values listed in ref 31 and presented in Figure 2. Given that $Cp^*Zn_2Cp^*$ is a stable

(30) Kaupp, M.; Von Schnering, H. G. *Inorg. Chem.* **1994**, *33*, 4718. Kaupp, M.; Von Schnering, H. G. *Inorg. Chem.* **1994**, *33*, 4179.

(31) The calculated reaction energies D_e (kcal·mol^{-1}) for reaction 1 are as follows (zero-point-corrected D_o values are given in parentheses): $CpBe_2Cp$, 67.6 (65.1); $CpBe_3Cp$, 30.8 (29.5); $CpBe_4Cp$, 29.3 (28.1); $CpBe_5Cp$, 29.3 (28.0); $CpMg_2Cp$, 14.2 (13.6); $CpMg_3Cp$, 3.9 (3.7); $CpMg_4Cp$, 3.8 (3.4); $CpMg_5Cp$, 3.9 (3.5); $CpCa_2Cp$, 9.6 (9.2); $CpCa_3Cp$, 3.4 (3.4); $CpCa_4Cp$, 3.5 (3.2); $CpCa_5Cp$, 3.9 (3.7); $CpZn_2Cp$, 22.5 (21.7); $CpZn_3Cp$, 4.9 (4.5); $CpZn_4Cp$, 1.9 (1.6); $CpZn_5Cp$, 1.6 (1.4).

(32) Rayón, V. M.; Frenking, G. *Chem.—Eur. J.* **2002**, *8*, 4693.

(33) (a) Fischer, E. O.; Hofmann, H. P. *Chem. Ber.* **1959**, *92*, 482. (b) Wong, C.; Wang, S. *Inorg. Nucl. Chem. Lett.* **1975**, *11*, 677. (c) Almenningen, A.; Bastiansen, O.; Haaland, A. *J. Chem. Phys.* **1964**, *40*, 3434. (d) Almenningen, A.; Haaland, A.; Lusztyk, J. *J. Organomet. Chem.* **1979**, *170*, 271. (e) Nugent, K. W.; Beattie, J. K.; Hambley, T. W.; Snow, M. R. *Aust. J. Chem.* **1984**, *37*, 1601.

(34) Chase, M. W. NIST-JANAF Thermochemical Tables, Fourth Edition. *J. Phys. Chem. Ref. Data* **1998**, Monograph 9, 1.

Table 2. Results of EDA at the BP86/T2ZP Level for Mono- and Dimetallocenes Using $(Cp^-)_2 + M_n^{2+}$ as Fragments: Energy Values (kcal·mol^{-1}), NBO Atomic Partial Charges $q(M_n)$, Distances between the Metal Atom and the Center of the Cp Ring r(M−X) (Å)

	Cp−M−Cp[a]				Cp−M−M−Cp			
M	Be	Mg	Ca	Zn	Be	Mg	Ca	Zn
ΔE_{int}	−780.9	−636.7	−549.0	−707.9	−671.6	−510.5	−448.2	−570.5
ΔE_{Pauli}	35.9	52.7	73.6	85.5	100.4	91.2	126.5	144.2
ΔE_{elstat}[b]	−483.2 (59.2%)	−493.6 (71.6%)	−477.9 (76.8%)	−533.6 (67.3%)	−473.5 (61.3%)	−454.8 (75.6%)	−436.3 (75.9%)	−505.6 (70.7%)
ΔE_{orb}[b]	−333.6 (40.8%)	−195.8 (19.9%)	−144.7 (23.2%)	−259.8 (32.7%)	−298.5 (38.7%)	−146.9 (24.4%)	−138.4 (24.1%)	−209.2 (29.3%)
ΔE_σ[c]	−117.5 (35.2%)	−65.5 (33.5%)	−34.5 (23.9%)	−116.1 (44.7%)	−93.6 (31.4%)	−52.5 (35.8%)	−42.6 (30.7%)	−84.5 (40.4%)
ΔE_π[c]	−186.3 (55.8%)	−106.6 (54.4%)	−92.6 (64.0%)	−117.5 (45.2%)	−181.4 (60.8%)	−79.0 (53.8%)	−84.8 (61.3%)	−106.1 (50.7%)
ΔE_δ[c]	−29.9 (8.9%)	−23.8 (12.2%)	−17.6 (12.2%)	−26.3 (10.1%)	−23.4 (7.8%)	−14.4 (10.4%)	−10.0 (8.0%)	−18.6 (8.9%)
$q(M_n)$[d]	+1.68	+1.74	+1.72	+1.60	+1.70	+1.80	+1.75	+1.85
r(M−X)	1.689	2.037	2.377	1.991	1.551	2.045	2.371	1.972

[a] Values are taken from ref 32. [b] The percentage values in parentheses give the contribution to the total attractive interactions $\Delta E_{elstat} + \Delta E_{orb}$. [c] The percentage values in parentheses give the contribution to the total orbital interactions ΔE_{orb}. [d] NBO analyses were done at the BP86/6-311G(d,p)//BP86/TZ2P level.

molecule in the solid state, one can now estimate the energy differences related to the intermolecular forces for $CpZn_2Cp$(s) and CpZnCp(s). The gas-phase reaction 1 for formation of $CpZn_2Cp$ is endothermic by $D_o = 21.7$ kcal·mol^{-1}. Since the sublimation energy of Zn is 31.2 kcal·mol^{-1}, it follows that a multimetallocene may still become isolated in the condensed phase even when reaction 2 is exothermic by ∼10 kcal·mol^{-1}. This means that diberyllocene (reaction energy for reaction 2, $\Delta E_R = -12.3$ kcal·mol) might also become isolated while dimagnesocene (reaction energy for reaction 2, $\Delta E_R = -21.6$ kcal/mol) and dicalcocene (reaction energy for reaction 2, $\Delta E_R = -33.3$ kcal·mol) are less likely to become synthesized in the condensed phase.[31] The reaction enthalpies of reaction 2 for the considered tri- to pentametallocenes are even more exothermic irrespective of the nature of the metal. It seems unlikely that the latter species may be identified in solution or in the solid state.

We analyzed the nature of the metal−ligand interactions in CpM_nCp with the EDA method. We first compare the results for the dimetallocenes CpM_2Cp with those of the parent systems CpMCp which have recently been studied by us in a comprehensive theoretical investigation of main-group metallocenes of groups 1, 2, 13, and 14.[32] The EDA data for CpM_2Cp and CpMCp are shown in Table 2.

The comparison of the EDA data for CpM_2Cp with the values for CpMCp indicates that the nature of the interactions between M_2^{2+} and $(Cp^-)_2$ is very similar to that of the interactions between M^{2+} and $(Cp^-)_2$. The atomic partial charges of M_2^{2+} are slightly more positive than for M^{2+}, but in both cases they are sufficiently close to +2 to justify the choice of the doubly charged fragments. Please note that the EDA values for CpMCp were calculated using the slightly smaller basis set TZP while the CpM_2Cp values were obtained using the TZ2P basis set. Our experience has shown that the EDA values do not differ very much between BP86/TZ2P and BP86/TZP.[28b] Also, the EDA analysis for CpMCp was carried out using optimized geometries which possess D_{5d} symmetry.[32] The D_{5h} and D_{5d} structures of CpMCp were found to be energetically nearly degenerate.

The total interaction energies ΔE_{int} between M_2^{2+} and $(Cp^-)_2$ are about 100−130 kcal·mol^{-1} less attractive than between M^{2+} and $(Cp^-)_2$ (Table 2). The EDA results suggest that all three energy terms contribute to the smaller ΔE_{int} values in the dimetallocenes; i.e., the Pauli repulsion ΔE_{Pauli} is larger and the electrostatic attraction ΔE_{elstat} and attractive orbital interactions ΔE_{orb} are smaller than in CpMCp. Table 2 shows that the distances M−X between the metal atoms and the center of the Cp ring in $CpCa_2Cp$ and $CpZn_2Cp$ are even slightly smaller than in the respective metallocenes CpCaCp and CpZnCp while the Mg−X distance in $CpMg_2Cp$ is a bit larger than in CpMgCp. It is interesting to note that the Be−X distance in $CpBe_2Cp$ is much shorter than in CpBeCp. Note that neither the D_{5h} nor the D_{5d} form is an equilibrium geometry of beryllocene. Geometry optimizations of CpBeCp yielded a slipped-sandwich structure with C_s symmetry which is, however, only <1 kcal·mol^{-1} lower in energy than the D_{5d} form.[32] The calculations of the geometry of beryllocene led to the conclusion that the molecule has a fluxional structure because the potential energy surface is very flat, which is in agreement with experimental observations.[33] Likewise, CpZnCp adopts a structure similar to that of CpBeCp, but in this case the energy difference with respect to the D_{5d} geometry is higher (ca. −3.7 kcal·mol^{-1}).[32]

From the above data it becomes obvious that the weaker metal−ligand interactions in CpM_2Cp compared with the bonding in CpMCp does not come from longer M−X distances. The EDA data provide a reasonable explanation for the finding. As mentioned before, the metal atoms in CpMCp can be considered as dications M^{2+}, which means that the valence shell of the atoms is empty. This explains the rather small values for the Pauli repulsion in CpMCp because they involve only the core electrons of the metals. The metal moiety in CpM_2Cp is the dimetal dication M_2^{2+}, which means that the energetically lowest lying σ orbital of M_2, which comes from the bonding combination of the (n)s orbitals of M, is occupied. There is now some Pauli repulsion between the occupied valence orbitals of the ligands and one occupied valence MO of the metal core in CpM_2Cp. The ocupation of one valence orbital in M_2 also shields the metal nuclei, which leads to less electrostatic attraction with the valence electrons of $(Cp^-)_2$. Finally, the acceptor strength of M_2^{2+} is less than that of M^{2+}, which yields weaker orbital interactions ΔE_{orb}. Table 2 shows that the breakdown of the ΔE_{orb} term into σ and π contributions gives smaller values for ΔE_σ and ΔE_π in CpM_2Cp than in CpMCp with the notable exception of the ΔE_σ contribution to the calcium compounds. This may be caused by an intrafragment relaxation effect. Note that the energy contributions of ΔE_δ that come from the polarization functions have a magnitude which may influence the change in the ΔE_σ and ΔE_π terms, which are the only genuine orbital contributions to the bonding.

The EDA results suggest that the natures of the metal−ligand bonds in CpM_2Cp and in CpMCp are not very different from each other. The binding interactions between M_n^{2+} and $(Cp^-)_2$ have a larger electrostatic than covalent character particularly for the magnesium, calcium, and zinc compounds. The metal−ligand bonding in the beryllocenes is a bit more covalent than in the other species, but the percentage contribution of ΔE_{elstat}

Table 3. Results of EDA at the Level BP86/TZ2P for Tri-, Tetra-, and Pentametallocenes Using $(Cp^-)_2 + M_n^{2+}$ as Fragments: Energy Values (kcal·mol^{-1}), NBO Atomic Partial Charges $q(M_n)$, Distances between the Terminal Metal Atom and the Center of the Cp Ring $r(M-X)$ (Å)

	M	Be	Mg	Ca	Zn
$n = 3$	ΔE_{int}	−597.0	−439.8	−393.3	−485.7
	ΔE_{Pauli}	155.2	121.8	158.5	168.9
	ΔE_{elstat}[a]	−467.2 (62.1%)	−424.2 (75.5%)	−411.6 (74.5%)	−468.4 (71.6%)
	ΔE_{orb}[a]	−285.0 (37.9%)	−137.5 (24.5%)	−140.8 (25.5%)	−186.1 (28.4%)
	ΔE_{σ}[b]	−100.3 (35.2%)	−58.3 (42.4%)	−54.2 (38.4%)	−79.6 (42.8%)
	ΔE_{π}[b]	−165.1 (58.0)	−67.2 (48.9%)	−77.6 (55.2%)	−92.3 (49.6%)
	ΔE_{δ}[b]	−19.6 (6.8%)	−12.0 (8.7%)	−9.2 (6.4%)	−14.3 (7.6%)
	$q(M_n)$[c]	+1.72	+1.83	+1.77	+1.90
$n = 4$	ΔE_{int}	−552.2	−396.2	−360.7	−430.7
	ΔE_{Pauli}	202.8	145.8	178.9	187.2
	ΔE_{elstat}[a]	−467.5 (61.9%)	−403.8 (74.5%)	−392.6 (72.8%)	−440.2 (71.2%)
	ΔE_{Orb}[a]	−287.5 (38.1%)	−138.2 (25.5%)	−146.9 (27.2%)	−177.6 (28.8%)
	ΔE_{σ}[b]	−112.6 (39.2%)	−66.9 (48.4%)	−65.0 (44.3%)	−82.5 (46.4%)
	ΔE_{π}[b]	−157. 1 (54.7%)	−60.9 (44.0%)	−73.6 (50.2%)	−83.2 (46.8%)
	Δ_{δ}[b]	−17.7 (6.1%)	−10.4 (7.6%)	−8.2 (5.5%)	−12.0 (6.8%)
	$q(M_n)$[c]	+1.73	+1.83	+1.77	+1.91
$n = 5$	ΔE_{int}	−522.1	−366.2	−338.0	−392.4
	ΔE_{Pauli}	243.7	165.3	194.1	202.0
	ΔE_{elstat}[c]	−471.6 (61.6%)	−389.6 (73.3%)	−379.0 (71.2%)	−419.2 (70.5%)
	ΔE_{Orb}[a]	−294.2 (38.4%)	−141.9 (26.7%)	−153.1 (28.8%)	−175.1 (29.5%)
	ΔE_{σ}[b]	−125. 2 (42.6%)	−75.6 (53.3%)	−74.3 (48.6%)	−87.5 (50.0%)
	ΔE_{o}[b]	−152. 4 (51.8%)	−57.0 (40.2%)	−71.0 (46.4%)	−77.0 (44.0%)
	ΔE_{δ}[b]	−16.6 (5.6%)	−9.4 (6.5%)	−7.6 (5.0%)	−10.5 (6.0%)
	$q(M_n)$[c]	+1.72	+1.83	+1.77	+1.91

[a] The percentage values in parentheses give the contribution to the total attractive interactions $\Delta E_{elstat} + \Delta E_{orb}$. [b] The percentage values in parentheses give the contribution to the total orbital interactions ΔE_{orb}. [c] NBO analyses were done at the BP86/6-311G(d,p)//BP86/TZ2P level.

to the total attraction is still higher (∼60%) than the contribution of ΔE_{orb}. The orbital interactions come mainly from the π donation of the higher lying pair of degenerate $(Cp^-)_2$ MOs into the vacant p(π) orbitals of the metal, while the donation from the lower lying totally symmetric π orbitals of $(Cp^-)_2$, which possess σ symmetry in the complexes, into the vacant σ orbitals of the metals is less important.

Figure 3 shows a qualitative orbital diagram for the interactions in a dimetallocene, CpM_2Cp, using the fragments $(Cp^-)_2$ and M_2^{2+}, where M is a main-group element. The diagram illustrates the orbital interactions, whose strengths are given by the EDA values. The bonding and antibonding combination of the p(σ) orbitals of M_2^{2+} are not shown because they contribute only little to the $a'_1(\sigma)$ and $a''_2(\sigma)$ interactions. The HOMO is an $a'_1(\sigma)$ orbital, which is mainly the σ_g orbital of the M_2^{2+} fragment. The orbital diagram for the extended homologues CpM_nCp with $n = 3-5$ looks very similar to the diagram for CpM_2Cp. The former species have one additional occupied σ orbital for each metal atom coming from the M_n^{2+} moiety, which changes very little after insertion into the sandwich structure.

Table 3 gives the EDA results for the tri-, tetra-, and pentametallocenes. There is a smooth trend of the ΔE_{int} values toward weaker metal−ligand interactions in CpM_nCp from $n = 1$ to $n = 5$. This is graphically shown in Figure 4. The partial charges $q(M_n)$ in Table 3 indicate that the metal moieties in CpM_nCp carry a positive charge of nearly +2. The trend of smaller ΔE_{int} values for longer chain metallocenes agrees with the continuous increase of the ΔE_{Pauli} values in CpM_nCp from $n = 1$ to $n = 5$ (Tables 2 and 3). Table 3 shows that the electrostatic term does not exhibit a uniform trend for all CpM_nCp species. The ΔE_{elstat} values for the beryllocenes slightly increase from $n = 3$ to $n = 5$, while the other metallocenes show a continuous decrease of the electrostatic attraction. The trend of the orbital interactions ΔE_{orb} is very interesting. Table 3 shows that the ΔE_{orb} values of CpM_nCp exhibit a small increase for M = Be, Mg, and Ca from $n = 3$ to $n = 5$ while the zincocenes exhibit a decrease. Inspection of the σ and π bonding contributions reveals that the ΔE_{σ} values for all systems show a smooth increase while the ΔE_{π} values decrease from $n = 3$ to $n = 5$.

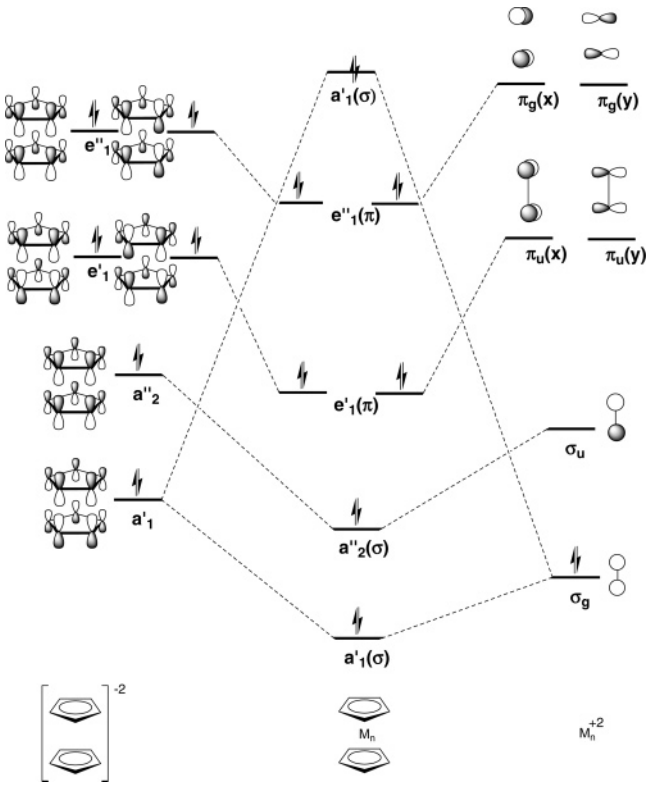

Figure 3. Qualitative orbital correlation diagram for dimetallocenes CpM_2Cp.

The nature of the metal−ligand bonding in terms of the percentage contribution of ΔE_{elstat} and ΔE_{orb} to the attractive interactions in the higher multimetallocenes is very similar to that in the lower members of the series. The covalent character of the bonds between M_n^{2+} and $(Cp^-)_2$ slightly increases from $n = 3$ to $n = 5$. The contributions of the σ interactions to ΔE_{orb}

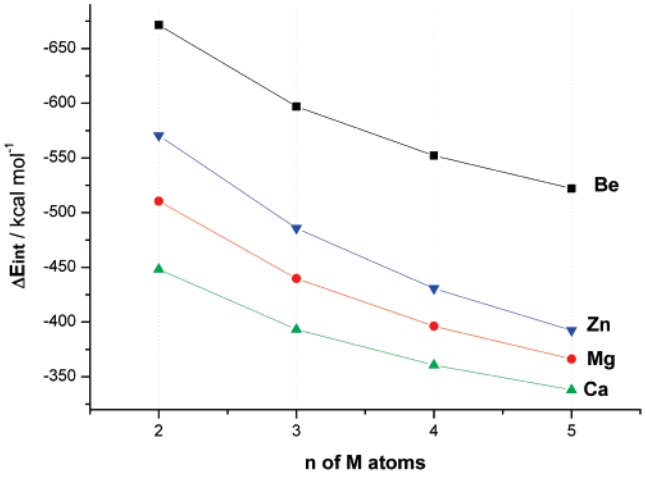

Figure 4. Trend of the interaction energies ΔE_{int} of CpM_nCp for $n = 2-5$.

continuously become larger while the π bonding becomes weaker when one goes from the trimetallocenes to the pentametallocenes.

Summary and Conclusion

The results of this work can be summarized as follows. The quantum chemical calculations of the multimetallocenes CpM_nCp with M = Be, Mg, Ca, and Zn show that species with $n > 2$ are thermodynamically unstable with respect to loss of one metal atom except for the beryllium species. The beryllocenes exhibit unusual stabilities for the whole series $CpBe_nCp$ up to $n = 5$. The calculations suggest that the energy for loss of one metal atom from $CpBe_2Cp$ is significantly higher than from $CpZn_2Cp$. The energy for the metal extrusion reaction of $CpBe_3Cp$ is much less endothermic than for $CpBe_2Cp$, but it is still more endothermic than the reaction of $CpZn_2Cp$. The thermodynamic stability of the higher members $CpBe_4Cp$ and $CpBe_5Cp$ toward loss of one metal atom in the gas phase is only slightly less than for $CpBe_3Cp$, while the other multimetallocenes, CpM_3Cp, CpM_4Cp, and CpM_5Cp (M = Mg, Ca, Zn), possess little extra stabilization with respect to the dimetallocenes. The calculated reaction energies for loss of one metal atom, which include the heats of sublimation of the metals, indicate that $CpBe_2Cp$ might become isolated in the condensed phase while the prospect for $CpCa_2Cp$ and $CpMg_2Cp$ and for the higher members CpM_3Cp, CpM_4Cp, and CpM_5Cp is less likely.

The analysis of the metal−ligand bonding in CpM_nCp using the EDA method suggests that the interactions between M_n^{2+} and $(Cp^-)_2$ have a larger electrostatic than covalent character. The beryllocenes are more covalently bonded than the other multimetallocenes. The orbital interactions in the lower members of CpM_nCp come mainly from π orbitals, but the σ contribution continuosly increases when n becomes larger and eventually may become stronger than the π contributions, which become weaker in the higher members of the series.

Acknowledgment. We are grateful for financial support from the Direccion de Investigacion y Posgrado (Dinpo) of Universidad de Guanajuato and the Deutsche Forschungsgemeinschaft. A.V. acknowledges Conacyt for a fellowship, and I.F. also acknowledges the Ministerio de Educación y Ciencia (Spain) for a postdoctoral fellowship.

Supporting Information Available: Cartesian coordinates (Å) and total energies (au) of all the multimetallocenes discussed in the text. This material is available free of charge via the Internet at http://pubs.acs.org.

OM700477B